

Probabilistic Direct Stability Assessment

Vladimir Shigunov, *DNVGL Maritime, Hamburg, Germany*, vladimir.shigunov@dnvgl.com

ABSTRACT

According to the Second Generation Intact Stability Criteria (SGISC), developed by IMO, assessment of dynamic intact stability of ships can be done using either of three “levels” of assessment: Levels 1 and 2 involve significant simplifications, whereas Level 3 is based on advanced numerical simulation methods and allows, in principle, using probabilistic measures directly as safety criteria. Because the number of stability failures per design life is very low (problem of rarity), and because reliable estimation of probabilistic measures requires multiple realisations, direct use of probabilistic measures requires very long simulation time. Two possible solutions for this problem are studied in the paper: one uses extrapolation of the mean time to stability failure over wave height, and the other the reduction of the total space of conditions encountered during the design life (sea states, wave directions and ship speeds) to a small number of selected situations (“design sea state approach”), which are supposed to adequately reflect the ship’s dynamic stability in all conditions. Accuracy and adequacy of these two approaches is checked in numerical simulations.

Keywords: *Intact Stability, Probabilistic Methods, Design Sea States*

1. INTRODUCTION

According to the framework of the Second Generation Intact Stability Criteria (SGISC), the ship design should fulfill (in each condition of loading) requirements of any of three assessment Levels (1, 2 or 3), Fig. 1. Alternatively, Operational Limitations (OL) or Operational Guidance (OG) can be developed, based on results of Level 2 or Level 3 assessment, respectively.

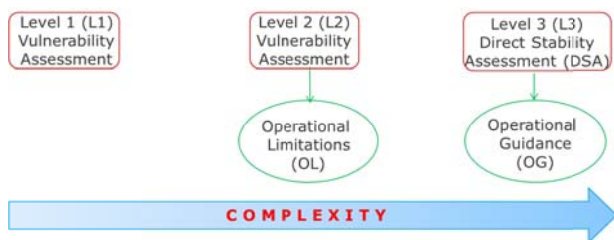


Figure 1: Second Generation Intact Stability Criteria.

Level 3, including Direct Stability Assessment (DSA) and Operational Guidance (OG), is based on direct numerical simulation of ship motions in waves and allows, in principle, using direct probabilistic measures of the likelihood of failure as safety criteria: probability of failure in given time or time to failure. Although direct numerical simulations have been already used by designers

and Classification Societies (e.g. for the definition of structural loads, dimensioning of cargo securing and lashing, passenger comfort assessment and accident investigation), and although SOLAS allows, in principle, their use as alternative design assessment methods for the evaluation of ship dynamic stability, practical approval by the Administrations requires definition of clear and uniform procedures, as well as availability of suitable tools.

What is the sense of going for Level 3 assessment when a ship (in a particular loading condition) fails to fulfill Level 1 and Level 2? Simplifications involved in Level 1 and Level 2 procedures lead to scatter of assessment results compared to the true performance, which has to be compensated by safety margins. The safety margins are adjusted in such a way that all vessels, passing Levels 1 and 2, are sufficiently safe (which means that vessels, not passing these assessment levels, are not necessarily unsafe). Better accuracy of DSA allows reducing safety margins, thus loading conditions, not fulfilling Level 1 and 2 assessments, may be evaluated as sufficiently safe by DSA. Moreover, loading conditions failing DSA may still be allowed as seagoing loading conditions if Operational Guidance is provided. This means increased payload and better operability.

Level 1 and Level 2 criteria are close to finalization [1]; work on DSA and OG is planned to be finished by SDC4 (February 2017). Therefore, DSA and OG should be discussed in detail until then; this paper provides input for such discussion.

2. PROBABILISTIC MEASURES

Either non-probabilistic (mean roll amplitude, maximum roll amplitude per specified exposure time, root-mean-square of roll angle etc.) or probabilistic measures can be used as safety criteria. When a probabilistic approach is used for DSA or OG, one possibility is to directly use the *probability of stability failure during a given exposure time* as a criterion. This probability can be found by direct counting, e.g. as (weighted over all sea states) number of stochastic realisations of each sea state in which stability failure occurred to the entire number of realisations.

Alternatively to directly using probability of stability failure during a given time, another probabilistic measure is frequently used, the *average time to stability failure*. It is convenient and common to assume stability failure events to be described as a stationary Poisson process (which can be done if stability failure events are independent of each other). One way to achieve the independence of stability failure events in simulations is by performing them only until the first stability failure event. For a Poisson process, the *time interval until stability failure* is a random variable, satisfying exponential distribution with a constant rate parameter r and

- probability density function

$$f(x; r) = re^{-rx} \text{ for } x \geq 0 \text{ and } 0 \text{ otherwise} \quad (1)$$

- cumulative distribution function

$$F(x; r) = 1 - e^{-rx} \text{ for } x \geq 0; 0 \text{ otherwise} \quad (2)$$

- average time until stability failure

$$E\{X\} \equiv \bar{T} = 1/r \quad (3)$$

- standard deviation of time until failure

$$\sigma\{X\} = 1/r = \bar{T} \quad (4)$$

- variance of time until stability failure

$$\text{Var}\{X\} = 1/r^2 = \bar{T}^2 \quad (5)$$

The probability of at least one failure during time t can then be calculated as

$$p = 1 - e^{-rt} = 1 - e^{-t/\bar{T}} \quad (6)$$

or, for small failure rates $r \ll \bar{T}$,

$$p \approx t/\bar{T} \quad (7)$$

The estimate of the average time until stability failure \bar{T} can be found by repetition of numerical simulations N times and averaging time intervals T_i until the first stability failure from each simulation,

$$\bar{T} \approx \tilde{T} = \frac{1}{N} \sum_{i=1}^N T_i \quad (8)$$

Figure 2 compares function $g(x) \equiv -\ln[1-F(x)]$ derived from numerical simulations with the function $g(x) \equiv -\ln[1-F(x)] = x/\bar{T}$ following, for exponential distribution, from eq. (2) for $x \geq 0$. Figure 3 plots standard deviation σ of time until failure event vs. the average time until failure \bar{T} in comparison with the theoretical line for exponential distribution $\sigma = \bar{T}$, following from (4). Figures 2 and 3 confirm the validity of assuming Poisson process for stability failures and exponential

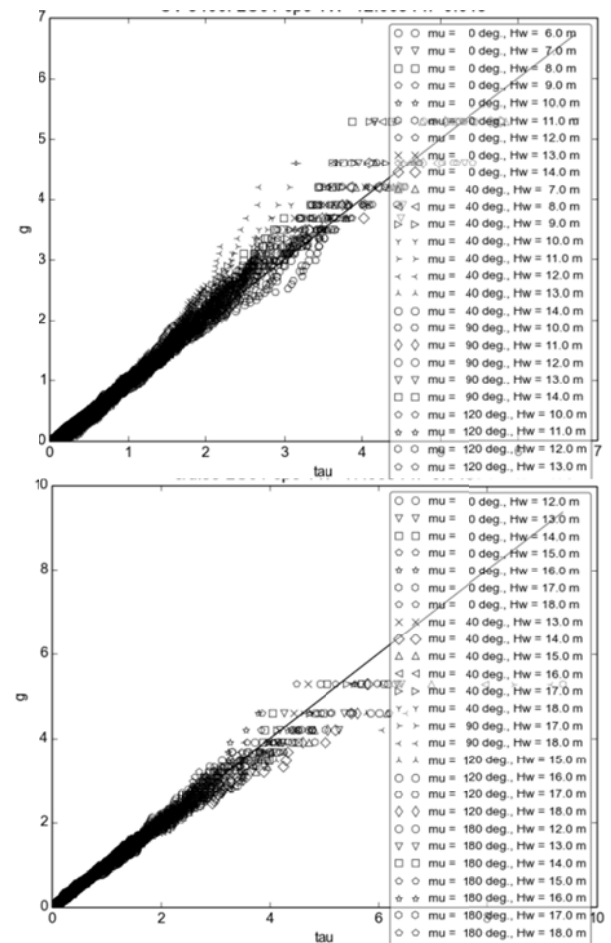


Figure 2: Function $g = -\ln(1-F)$ (y-axis) vs. non-dimensional time until stability failure $\tau = T/\bar{T}$ (x-axis) from numerical simulations (symbols) and theoretical exponential distribution (2) (line) for a container ship (top) and a cruise vessel (bottom).

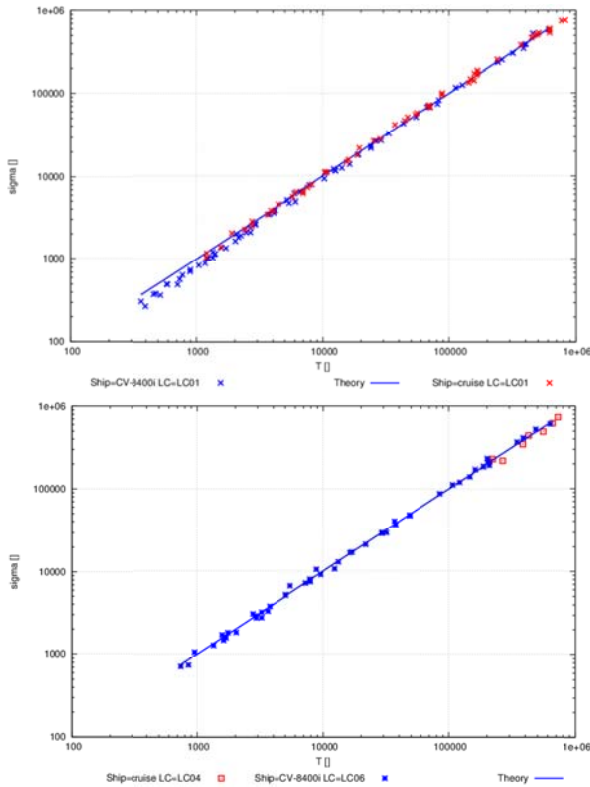


Figure 3: Standard deviation of time until stability failure (y-axis) vs. average time until stability failure \tilde{T} (x-axis) from numerical simulations (symbols) and theoretical exponential distribution (4) (line) for exceedance of 40° roll angle (top) and 6.3 m/s^2 lateral acceleration (bottom).

distribution for time interval until stability failure, if care is taken in numerical simulations that stability failure events are independent of each other.

Although stability failure has not been defined yet within the Second Generation Intact Stability Criteria, an obvious definition is an exceedance of some roll angle or lateral acceleration threshold. In the examples considered here, exceedance of roll angle of 40° or lateral acceleration of 6.3 m/s^2 was used for illustration.

A practically relevant question is the required number of stability failure events to be encountered in simulations for an accurate enough estimate \tilde{T} of the average time until stability failure \bar{T} . The standard deviation σ_m of the mean time until stability failure \bar{T} satisfies, for large enough N , the law of large numbers

$$\sigma_m = \sigma / \sqrt{N} \quad (9)$$

where σ is the standard deviation of the time until stability failure. Using $\sigma = \bar{T}$ according to (4) for exponential distribution and requiring 95% confidence for the estimate \tilde{T} leads to the half-breadth of the 95%-confidence interval equal to

$$\Delta T = 1.96\sigma_m = 1.96\tilde{T}/\sqrt{N};$$

thus, the required number of stability failure events

$$N = 1.96^2 / (\Delta T / \tilde{T}) \quad (10)$$

Figure 4 shows the 95% confidence interval ΔT as percentage of \tilde{T} depending on the number of stability failure events N ; $N=100$ and 200 correspond to about 20 and 13% error, respectively.

3. PROBLEM OF RARITY

Using probabilistic safety measures as criteria requires some form of counting of stability failures, which means that stability failure events should be really encountered during numerical simulations. For the cases of interest in practical approval, the typical number of stability failure events per design life is very low: of the order of magnitude of less than one per design life (about 30 years), which means that the relevant average time until stability failure in simulations is more than 30 years.

Besides, accurate estimation of average time to failure from numerical simulations requires many repetitions of simulations in multiple random realisations of sea states: about 200 according to Fig. 4, if 10%-accuracy is required. This means, however, very long simulation time: for the considered 30 years and 200 realisations, 6000 years of simulation time.

Even with significantly simplified numerical simulation methods, achieving, for example, 1/1000 ratio of computation time to the simulation time, the resulting computational effort is too large. Below, two procedures are proposed that can significantly reduce computational time.

4. NUMERICAL TOOLS AND EXAMPLES

In the examples below, numerical simulations were carried out with a seakeeping simulation tool *rolls* [2], combining linear hydrodynamics with

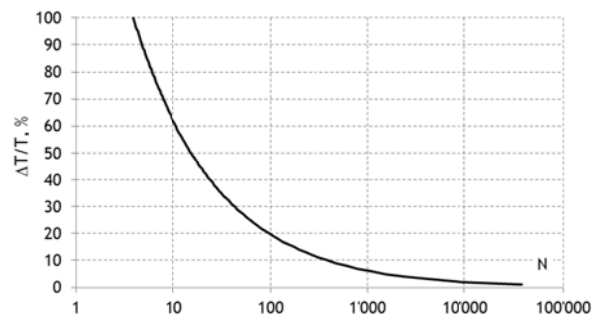


Figure 4: 95% confidence interval ΔT as percentage of \tilde{T} vs. the number of stability failure events N .

nonlinear Froude-Krylov and restoring forces, which is about 10^3 times quicker than real time for motion simulations in irregular short-crested waves.

As example ships, a cruise vessel, 1700, 8400 and 14000 TEU container ships and a RoRo ferry were used. For each vessel, three low-*GM* loading conditions were selected, for illustration of the pure loss, parametric roll and dead ship condition stability failure modes, and three high-*GM* loading conditions to illustrate excessive accelerations stability failure mode, Fig. 5.

5. EXTRAPOLATION OF FAILURE RATE OVER WAVE HEIGHT

To reduce the total simulation time required for probabilistic direct stability assessment and probabilistic operational guidance, extrapolation of

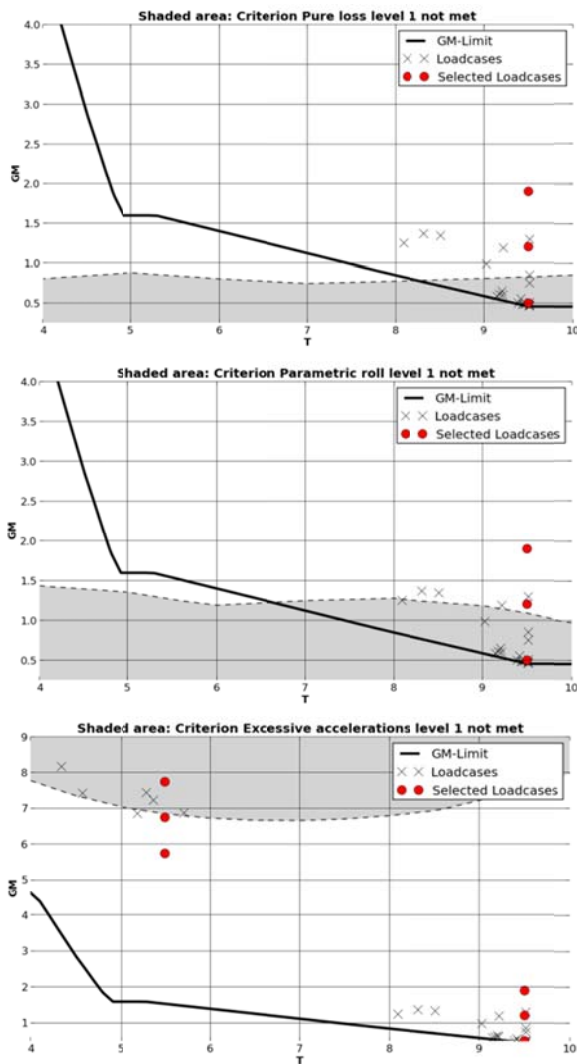


Figure 5: Loading conditions in example computations (●) for 1700 TEU container ship: draft (x-axis) vs. *GM* (y-axis), minimum *GM* according to 2008 IS Code (—), Level 1 vulnerability areas (grey) for pure loss (top), parametric roll (middle) and excessive accelerations (bottom) and loading conditions from Trim and Stability Booklet (x).

stability failure rate r or average time until stability failure $T=1/r$ over wave height (at the same wave period) can be used. This approach can be used to efficiently take into account all sea states in a scatter table, thus, if this method is applied for direct stability assessment, the results can be directly used as operational guidance.

The extrapolation method, proposed first by Tonguc and Söding [3], is applied here in the following form:

$$\ln T = A + B/h_s^2 \tag{11}$$

where T is the average time until a stability failure, h_s is the significant wave height, and A and B are constants, independent from the significant wave height but depending on wave period and direction, ship speed and loading condition.

A linear extrapolation of $\ln T$ over $1/h_s^2$ can be performed for such values of $\ln T$, for which $\ln T$ linearly depends on $1/h_s^2$, see e.g. Fig. 6. Note that linear extrapolation is also acceptable when the dependency of $\ln T$ on $1/h_s^2$ is convex, as in the example in Fig. 7; linear extrapolation in such cases leads to under-estimation of the average time until stability failure, i.e. to conservative results.

To find a value of $\ln T$, at and above which linear extrapolation over $1/h_s^2$ can be performed (in an accurate or at least conservative way), series of numerical simulations were performed for all ships and loading conditions described above at various forward speeds and seaway periods and directions. For each of these combinations, significant wave height was systematically varied. The average time until stability failure was defined from $N = 200$

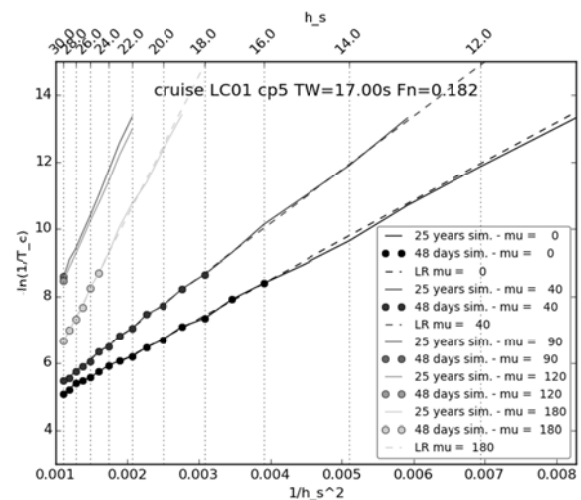


Figure 6: Examples of extrapolation approximating well results of direct simulations.

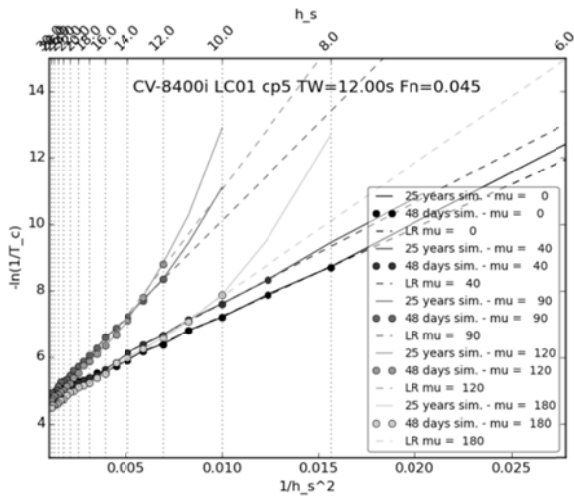


Figure 7: Examples of extrapolation leading to conservative results.

realisations of the same sea state until the first stability failure event (exceedance of 40° roll angle was used as stability failure event). The results of this study show that

- For most situations, the dependency of $\ln T$ on $1/h_s^2$ becomes linear for $\ln T > 5$, Fig. 8.

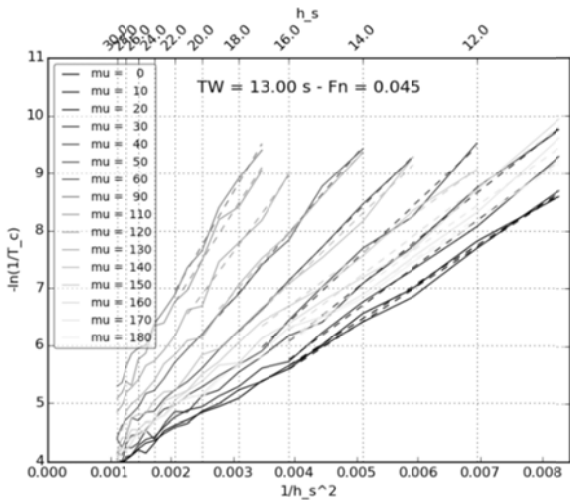


Figure 8: Examples of linear dependency of $\ln T$ on $1/h_s^2$ over complete range of wave heights.

- In many situations, the dependency of $\ln T$ on $1/h_s^2$ is slightly to moderately convex, Fig. 9 (top), in some cases strongly convex, Fig. 9 (bottom); for such cases, linear extrapolation of $\ln T$ over $1/h_s^2$ for $\ln T > 5$ would lead to conservative results, i.e. is still acceptable.
- In some situations, the dependency of $\ln T$ on $1/h_s^2$ is concave for $\ln T < 6$, Fig. 10; in such cases, extrapolation can be performed for $\ln T > 6$ to avoid non-conservative errors.

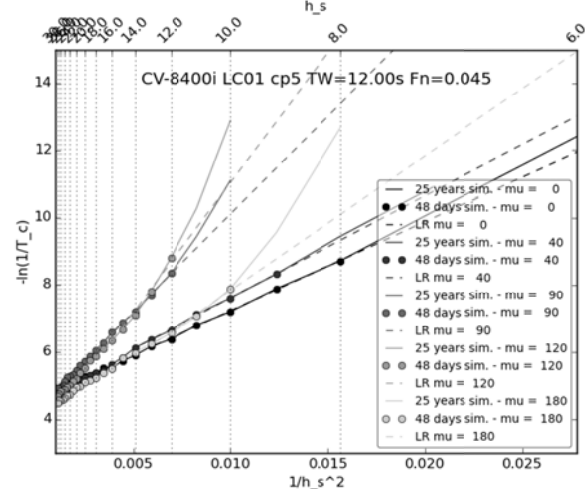
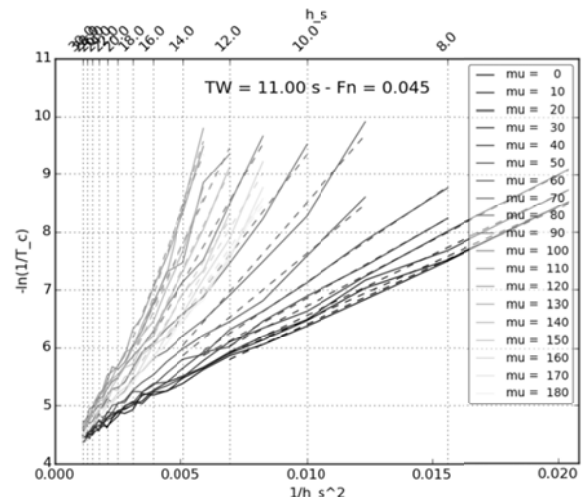


Figure 9: Examples of convex dependencies of $\ln T$ on $1/h_s^2$; linear extrapolation is conservative.

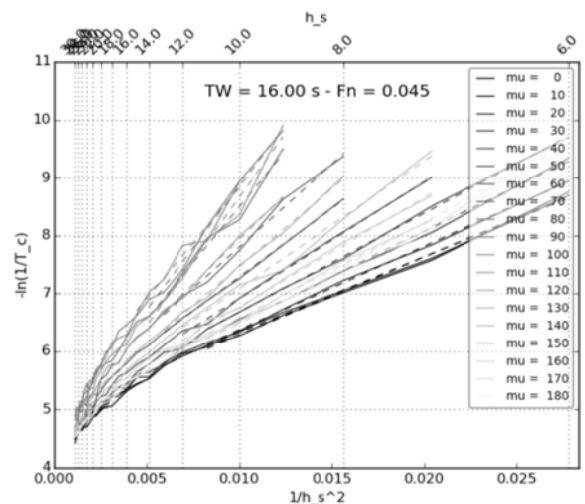


Figure 10: Concave dependencies of $\ln T$ on $1/h_s^2$ for $\ln T < 6$; linear extrapolation can be used for $\ln T > 6$.

Note that $\ln T = 6$ means about 400 s time interval until stability failure, which is feasible for modern numerical simulation methods.

If extrapolation of failure rate (or time interval until failure) over wave height is used, the required number of failure events used for averaging at each wave height can be reduced, because linear extrapolation can be simultaneously used as a smoothing linear fit to remove stochastic oscillations. Figure 11 compares dependencies of $\ln T$ on $1/h_s^2$, obtained with 200 (solid lines) and 20 (dashed lines) realisations per point. Although dashed lines show more stochastic oscillations, they can still be used for a linear fit.

For loading conditions, marginally fulfilling Level 1 parametric roll vulnerability criteria, direct simulations can cover rather large part of a scatter table in a feasible simulation time. Such sea states are highlighted green in the example (North Atlantic scatter table) in Fig. 12; sea states for which extrapolation over wave height had to be used are highlighted blue.

6. DESIGN SEA STATES

Probabilistic direct stability assessment requires summation of short-term probabilities of stability failure over all sea states in a scatter table and over all seaway directions. For example, the IACS scatter table for the North Atlantic contains 197 non-zero entries; if assessment is performed for every 10° seaway directions, the number of short-term simulations becomes 3743 (for each forward speed and for each loading condition). One possibility to reduce the required number of short-term assessments is to reduce the total space of conditions encountered during design life (wave height, period and direction and ship speed) to a small number of representative situations, assumed to be sufficient for norming: ships performing well enough in the selected situations will also perform well enough in all possible conditions (“design sea states” method).

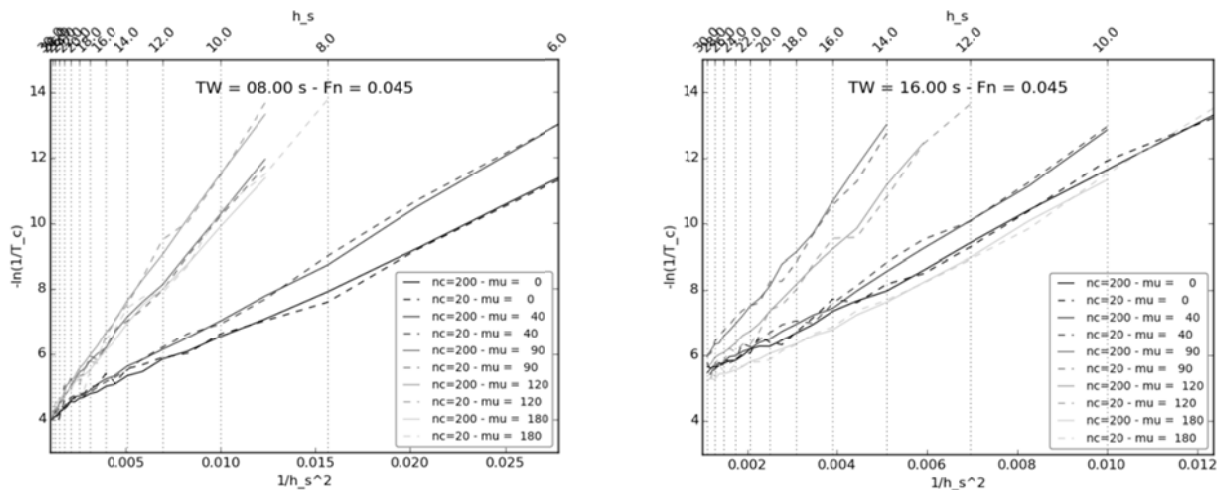


Figure 11: Examples of dependencies of $\ln T$ on $1/h_s^2$ using $N=200$ (solid lines) and 20 (dashed lines) realisations for a cruise vessel (left) and a 8400 TEU container ship (right).

HS/Tz	2	3	4	5	6	7	8	9	10	11	12	13	14	15	16	17	18
16										0.3	0.4	0.4	0.3	0.2			
15									0.5	1.0	1.3	1.2	0.7	0.3	0.2		
14								0.4	1.5	3.0	3.6	2.9	1.8	0.8	0.3		
13						0.1	1.4	4.6	8.3	9.1	6.9	3.9	1.8	0.6	0.2		
12						0.7	4.5	13.5	21.9	22.0	15.4	8.1	3.5	1.2	0.3		
11						2.3	14.0	37.4	54.3	49.9	32.1	15.7	6.2	2.0	0.6	0.2	
10					0.2	7.9	41.5	97.4	126.2	104.7	61.7	27.9	10.3	3.2	0.9	0.2	
9					2.1	26.1	116.3	237.0	271.9	202.7	108.8	45.2	15.5	4.5	1.1	0.3	
8					7.8	82.2	305.2	533.3	536.5	357.0	173.4	66.0	20.8	5.6	1.4	0.3	
7					0.3	29.0	243.2	740.5	1095.1	955.6	562.4	245.5	85.1	24.7	6.2	1.4	0.3
6					4.1	103.6	667.6	1633.6	2012.3	1503.4	774.4	301.1	94.4	25.1	5.9	1.2	0.3
5					19.0	347.4	1664.3	3193.7	3212.1	2021.5	899.0	307.9	86.4	20.8	4.5	0.8	0.1
4				0.5	88.6	1064.7	3641.5	5304.3	4240.3	2198.2	828.4	245.9	61.0	13.2	2.5	0.4	
3				9.0	386.5	2840.3	6542.8	6894.4	4207.4	1735.8	538.0	134.9	29.0	5.6	1.0	0.1	
2			0.1	72.1	1457.4	5780.8	8104.1	5669.4	2452.7	754.8	181.8	36.7	6.6	1.0	0.1		
1			1.5	291.4	1815.4	2811.2	1820.4	665.5	165.2	31.3	5.2	0.4					

Figure 12: Sea states in which failure rate was defined direct from numerical simulations (green) or extrapolated over wave height (blue); numbers correspond to frequency of occurrence of sea states in North Atlantic wave climate.

Various definitions of design sea states are possible; here design sea states cover all zero-upcrossing periods of a scatter table (with a step of 1 s), but with only one significant wave height per wave period; this wave height was defined using the wave steepness table from [3]. Three wave directions (head, beam and following) were used in each design sea state to cover parametric and synchronous roll and pure loss of stability.

For comparison, also full probabilistic direct stability assessment was performed, taking into account all zero-upcrossing seaway periods and all wave heights in the North-Atlantic scatter table and for all wave directions (assuming them uniformly distributed) with 10° step. Exceedance of 40° roll angle was used as stability failure. Note that in the full probabilistic assessment, it is not possible to separate contributions from parametric or synchronous roll or pure loss of stability in the total probability of stability failure.

The aim of this study was to compare results of full probabilistic stability assessment (full scatter table, all wave directions) with the assessment in design sea states (about 10 sea states, three wave directions). Stability failure rates in design sea states were weighted and summed; the weights were taken equal to the occurrence frequencies of zero-upcrossing periods. This assessment was performed for the same ships and loading conditions as in the previous section, separately at several forward speeds.

Using significant wave heights according to the wave steepness table [4] leads to relatively steep seaways. Still, stability failure rates could not be computed directly in some cases (particularly in short waves) because of too rare stability failure events; in such cases, extrapolation of stability failure rate over significant wave height was used. Examples in Fig. 13 illustrate this: the significant wave heights according to [3] are shown with vertical blue lines. In less steep sea states, e.g. as those suggested by Italy for Level 2 vulnerability assessment for parametric roll, stability failure events are much less rare and might require extrapolation at all wave periods. On the other hand, steeper design sea states than those according to [3] may be difficult to implement in model tests.

Figure 14 compares the dependencies of the weighted stability failure rate in design sea states

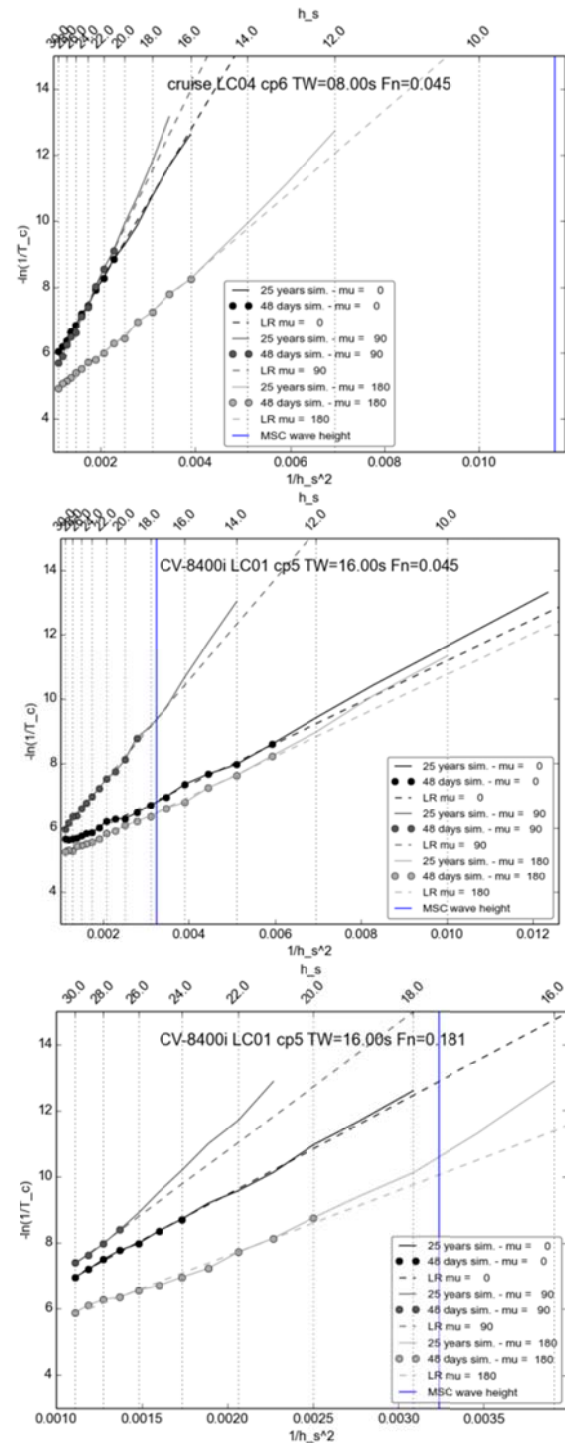


Figure 13: Examples of dependencies of $\ln T_c$ on $1/h_s^2$ in design sea states; vertical blue lines correspond to wave height according to seaway steepness table from [3].

(y-axis) on the long-term stability failure rate in all sea states and all wave directions (x-axis) for the four vessels between following, beam and head waves. Figure 15 shows weighted sums of stability failure rates over all design sea states (y-axis) vs. long-term stability failure rate in all sea states and all wave directions (x-axis) between the four vessels, each point corresponds to a combination of a loading condition and forward speed.

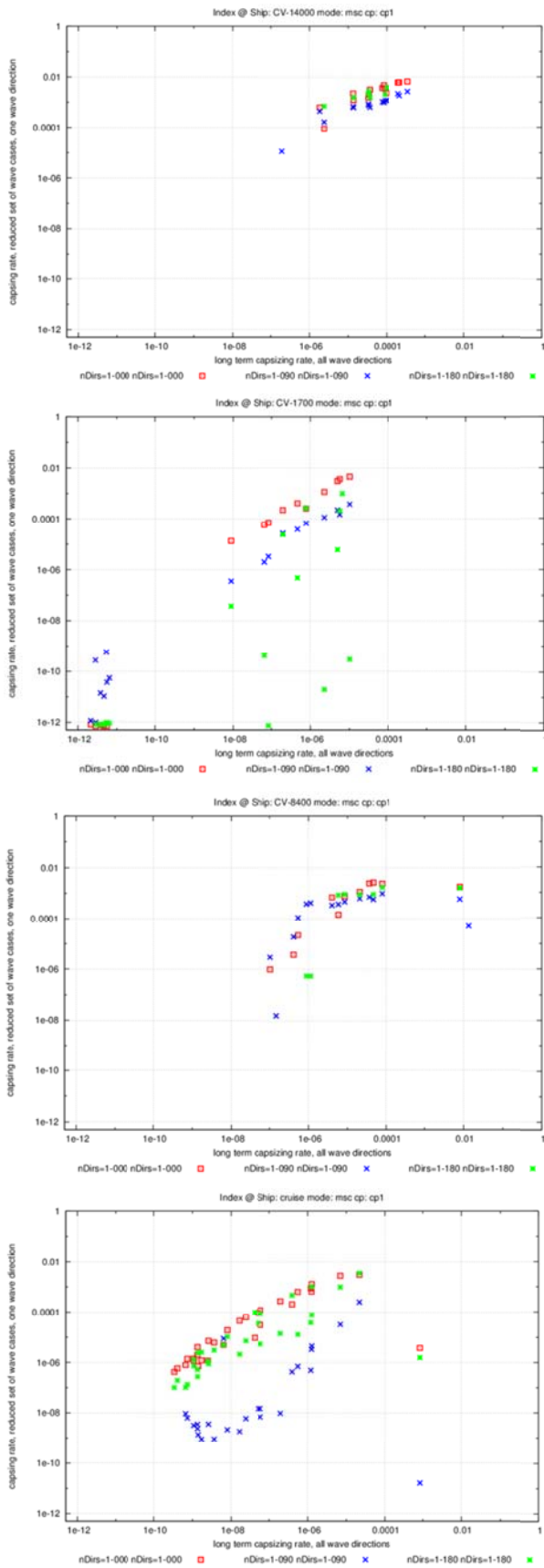


Figure 14: Stability failure rates in design sea states (y-axis) at three wave directions (different symbols) vs. long-term stability failure rate in all sea states and all wave directions (x-axis) for four vessels.

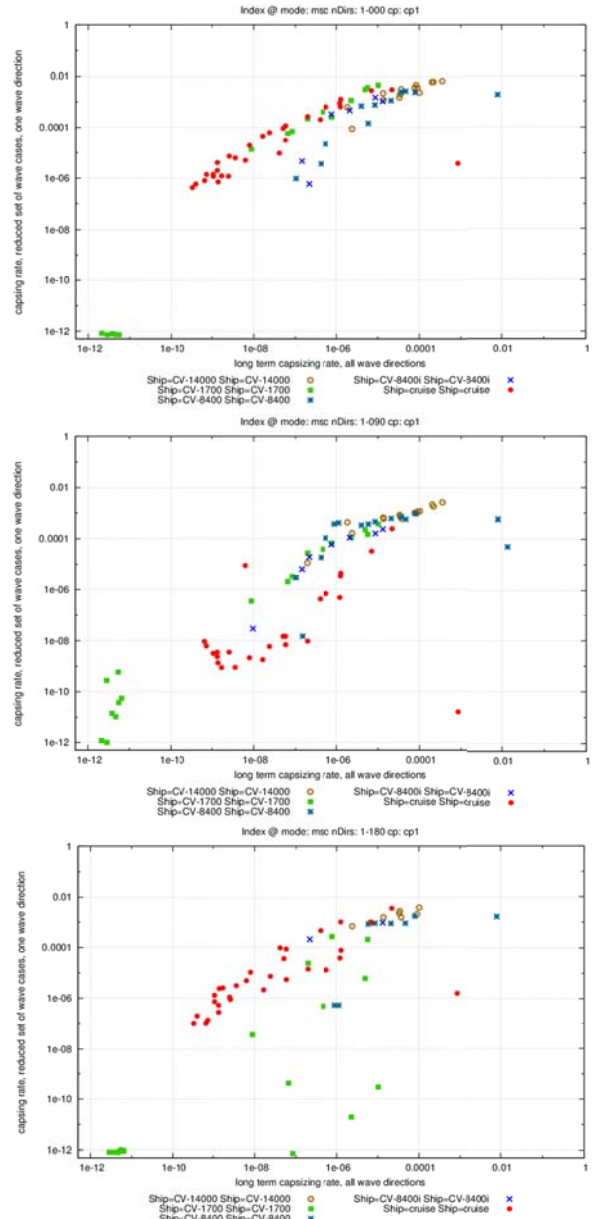


Figure 15: Stability failure rates in design sea states (y-axis) vs. long-term stability failure rate in all sea states and all wave directions (x-axis) for four vessels (different symbols) in following (top), beam (middle) and head (bottom) waves.

A similar comparison was performed for excessive accelerations stability failure mode for loading conditions with large initial GM values. The stability failure was defined as the exceedance of 6.3 m/s^2 lateral acceleration; simulations in design sea states were performed only in beam waves (long-term probabilistic assessment was still performed in all wave directions). Figure 16 shows the weighted sum of stability failure rates in design sea states in beam waves (y-axis) vs. the long-term excessive accelerations stability failure rate (x-axis) separately for each of the four vessels; Fig. 17 summarises results.

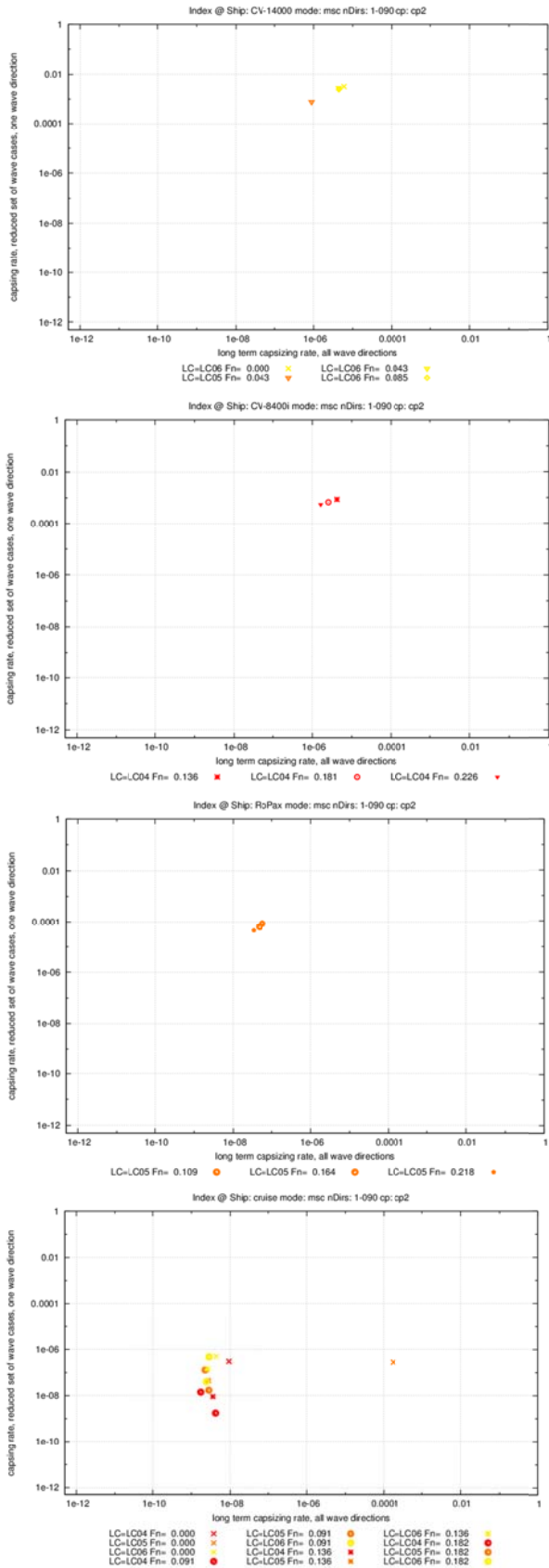


Figure 16: Excessive acceleration stability failure rate in beam design sea states (y-axis) vs. long-term stability failure rate in all sea states and all wave directions (x-axis) separately for each of four vessels.

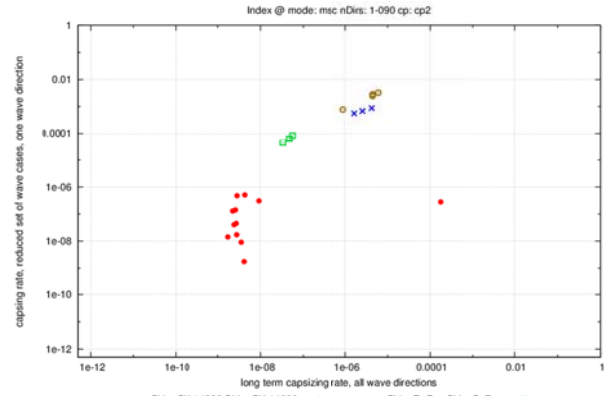


Figure 17: Excessive acceleration stability failure rate in beam design sea states (y-axis) vs. long-term stability failure rate in all sea states and all wave directions (x-axis) for four vessels (different symbols).

The concept of design sea states can be used if the dependency of the full long-term stability failure rate on the stability failure rate defined in design sea states is monotonous (i.e. ranking of different loading conditions is the same in the full long-term assessment and in the design sea states) and, besides, the same for all ships and all loading conditions. Figures 15 and 17 confirm, in principle, that this dependency is approximately monotonous, i.e. ranking of ships, loading conditions and forward speeds is correctly reproduced. However, these dependencies show significant scatter between ships and forward speeds, which means that standards, defined for the “design sea states” method will have to be selected conservatively for some ships, i.e. that this assessment is not the “true Level 3” assessment. This scatter requires further consideration, e.g. the idea of different design sea states for different stability failure modes may provide better results.

For the loading conditions on the margin of Level 1 vulnerability assessment, short-term stability failure rate in design seaways is of the order of $5 \cdot 10^{-3}$ 1/s in full scale; this corresponds to time until stability failure of about 30 s in model scale, which is feasible for model tests as well as for numerical simulations.

7. PRACTICAL CONSIDERATIONS

The preparation of the simulations has required about 2 days for 5 ships (6 loading conditions for each). Note that the required input is not part of standard approval, thus the preparation has required much manual work, which will not be required in

the future. The computation time per loading condition per forward speed was 750 h processor time for the full long-term assessment using extrapolation of failure rate over wave height. When design sea states assessment was used, the entire computational time was 68 h per loading condition per forward speed. Note that the reduction of the computational time of the design sea states method compared to the full assessment was only $750/68 \approx 11$ times, from which $19/3 \approx 6$ times due to the reduced number of wave directions; thus, the reduction of computing time due to the reduced number of wave heights (1 in the design sea states method vs. 16 in the full assessment) was only 1.7 times.

Extrapolation of stability failure rate over wave height in a probabilistic direct stability assessment can be applied to provide accurate or at least conservative results in acceptable computational time. The advantage of this approach is that the results of direct stability assessment can be directly used as operational guidance. On the other hand, design sea states approach can reduce the total computational time required for direct stability assessment by more than 10 times compared to the method based on extrapolation. Although the results of assessment in design sea states cannot be used as operational guidance, this method can be used to sort out sufficiently safe loading conditions at a lower computational cost, and then use a more comprehensive method to develop operational guidance only for those loading conditions that fail direct assessment.

Operational Guidance is defined as “*the recommendation, information or advice to an operator aimed at decreasing the likelihood of failures and/or their consequences*” [5]; it is assumed to be developed using outcomes of the direct stability assessment. Operational Guidance can be implemented, in principle, according to the following approaches: (1) pre-computation and approval of Operational Guidance at the design stage; (2) pre-computations by an on-shore provider before departure; and (3) real-time computations during operation.

Following option (1) Operational Guidance is pre-computed and approved in the design stage, which allows using most comprehensive numerical tools and statistical procedures, e.g. probabilistic assessment. However, such computations can be

performed only for assumed input parameters, most importantly, standard seaway spectra. Sensitivity of the results to the input parameters needs to be investigated. In option (2), Operational Guidance is pre-computed by an on-shore provider before departure from the port, using the most actual weather forecast available. This approach allows, in principle, using comprehensive numerical tools and statistical procedures. The drawback of this option is the possibility of unforeseen delays in the ship operator time schedule. In option (3), required computations are performed in real-time (on board or onshore) during operation, once accurate weather forecast is available, thus both numerical tools and statistical procedures have to be significantly simplified; note that the advantage of more accurate weather data may be to some degree compensated by reduced accuracy of numerical tools and statistical procedures. Note also that “real time” means here simulations well before encountering heavy weather conditions, in order to enable route changing to avoid heavy weather if operational measures are not sufficient to achieve the required safety level.

Input from all interested stakeholders is required to discuss advantages and drawbacks of options (1)-(3).

Finally, practical approval of Level 3 procedures (both direct stability assessment and operational guidance), needs quantification of the uncertainty of the proposed methods, both for the full assessment based on the extrapolation over wave height and for the design sea states method.

REFERENCES

- [1] IMO (2015) Report of the Working Group on Intact Stability SDC 2/WP.4, Annex 5
- [2] H. Söding, V. Shigunov, T. Zorn and P. Soukup (2013) Method *rolls* for simulating roll motions of ships, *Ship Technology Research – Schiffstechnik* **60**(2)
- [3] E. Tongué and H. Söding (1986) Computing capsizing frequencies of ships in seaway, *Proc. 3rd Int. Conf. on Stability of Ships and Ocean Vehicles*
- [4] IMO-MSC (2006) Interim Guidelines for alternative assessment of the Weather Criterion, MSC.1/Circ.1200
- [5] IMO (2008) Revision of the Intact Stability Code - Report of the Working Group (Part 1) SLF 51/WP.2, Annex 2